PHY 982 Homework 2

John Ash, Mengzhi Chen, Tong Li, Jason Surbrook

Feburary 27, 2018

1 Elastic Scattering between nucleons and ^{208}Pb

1.1 Coulomb scattering

In the case of point-Coulomb scattering, the Coulomb interaction between the projectile and the target with charges Z_1 and Z_2 is

$$V_c(R) = \frac{Z_1 Z_2 e^2}{R^2}, \tag{1}$$

where R is the distance between them. The Schrödinger's equation with this potential can be solved analytically. Related discussions are detailed in Ref.[1]. In sum, the angular distribution of point-Coulomb potential is described by the differential cross section

$$\sigma(\theta) = \frac{\eta^2}{4k^2 \sin^4(\theta/2)};\ \eta = \frac{Z_1 Z_2 e^2}{\hbar} \left(\frac{\mu}{2E}\right)^{\frac{1}{2}}, \tag{2}$$

where μ is the reduced mass and k is the wave number with the energy E. It worth noticing that the Eq. 3 is the same as the classical *Rutherford cross section*.

When the finite size of the target is included, due to different charge distributions, the interaction between the projectile and the target becomes more complicated. The case for uniform distribution over a sphere are formulated in Ref. [1].

Normally, these potentials are not analytically solvable. Sometimes, we can apply the *plane wave Born approximation* (PWBA) for the Coulomb scattering. Under PWBA, the differential cross section is

$$\sigma(\theta) = \frac{\eta^2}{4k^2 \sin^4(\theta/2)} \left|F(\theta)\right|^2, \tag{3}$$

where $F(\theta)$ is called the *form factor* related with the charge distribution as

$$F(\theta) = \int e^{i(\vec{k}_f - \vec{k}_i)\cdot\vec{r}'} \rho(r') d^3 r'. \tag{4}$$

In sum, we see the finite size of the target can give cross sections different from the point-like case.

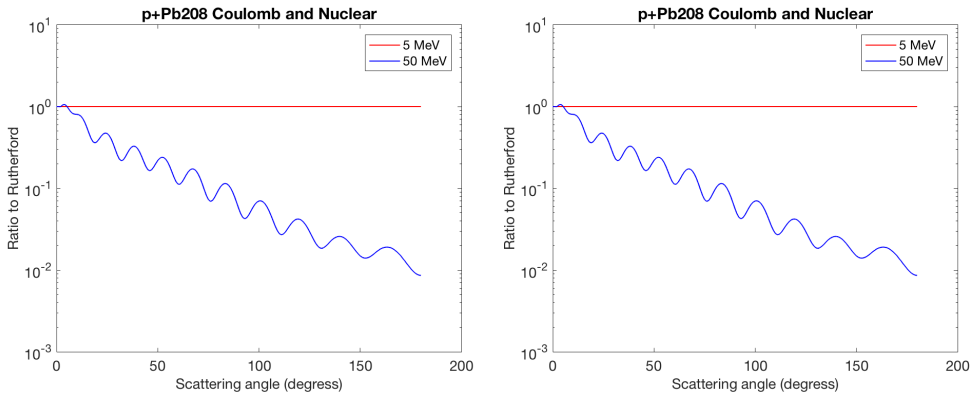

Figure 1: Differential cross sections for nucleons scattering with ^{208}Pb at 5 and 50MeV. Left panel is proton and right panel is neutron

1.2 The optical potential

In this section, we study the elastic scattering between nucleons and the ^{208}Pb target with the help of FRESCO[2] . Their effective interaction refers to as the optical potential. We take the global parameterization from Ref. [3, 4] as the input for FRESCO.

In the first step, we take two lab energies 5 and 50 MeV in our calculation. The results are shown in Figure 1. It gives the angular distributions in center of mass for protons and neutrons are shown. For the 5 MeV proton, the curve agrees well with the *Rutherford cross section*. Given that the radius parameter of optical potential is $r_w \sim 1.2\ fm$, we can estimate the Coulomb barrier for a proton to overcome. It should be

$$E_{Coul} \approx \frac{Z_1 Z_2 e^2}{r_w + R_2} \approx 15 \text{ MeV}. \tag{5}$$

We see that 5 Mev is much lower than the Coulomb barrier. Thus, this scattering can be referred as a point-like Coulomb scattering properly. The agreement with the *Rutherford cross section* also verifies this point. As going to 50 MeV which is strong enough to overcome the Coulomb barrier, the effective interaction plays a role and induces a diffraction pattern in Figure 1. In order to explore the influence of the optical potential, we will use $E_{lab} = 50$ MeV in our following calculations.

In our next step, we would like to see the influences of the depth of optical potential's imaginary part of the S-matrix. Fixing other parameters, we scale the depth of imaginary parts V_i (including volume, surface derivative and spin-orbit potentials) a factor of 1.5, 0.5 and 0. The modules of S-matrix with for the proton and the neutron are shown in Table 1 and 2. We can see that as we lower the depth, $|\mathbf{S}|^2$ gradually converges to one which indicates an elastic scattering. It inspires us that the imaginary parts describe absorptions in scattering processes. It also worth noticing that we don't see the growth of $|\mathbf{S}|^2$ with decreasing V_i in every partial waves. We suggest more information about total

Proton partial waves					
L	J	$\|\mathbf{S}\|^2(\bar{V}$=1.5)	$\|\mathbf{S}\|^2(\bar{V}$=1.0)	$\|\mathbf{S}\|^2(\bar{V}$=0.5)	$\|\mathbf{S}\|^2(\bar{V}$=0.0)
0	0.5	6.45E-04	2.33E-04	1.56E-02	1.0
1	0.5	9.17E-04	1.17E-03	1.63E-02	1.0
2	1.5	8.33E-04	1.28E-04	1.34E-02	1.0
1	1.5	9.19E-04	1.23E-03	1.74E-02	1.0
2	2.5	7.97E-04	1.17E-04	1.52E-02	1.0
3	2.5	1.27E-03	1.64E-03	1.81E-02	1.0
4	3.5	1.51E-03	2.89E-04	1.02E-02	1.0
3	3.5	1.27E-03	1.85E-03	2.11E-02	1.0
...	...	...	...	...	...

Table 1: The modules of S-matrix for proton partial waves with varying imaginary potentials, where $\bar{V}$ is the scaled depth defined as $\frac{V_i(new)}{V_i(old)}$.

absorptive cross sections for being fully convinced.

Moreover, we are interested in the effects of different radius parameters. Again, fixing other parameters, we repeat our calculations by scaling the radius parameters r (including volume, surface derivative and spin-orbit potentials) a factor of 0.2, 0.5, 2, 3 and 4. The results are shown in Figure 2. For the proton, we observe the dramatic up-down shifts and denser diffraction patterns with increasing r. It's the synergistic effect by the Coulomb and optical potentials. As for neutron, the changing of pattern is relative small as it only feels the optical potential.

Neutron partial waves					
L	J	$\|\mathbf{S}\|^2(\bar{V}$=1.5)	$\|\mathbf{S}\|^2(\bar{V}$=1.0)	$\|\mathbf{S}\|^2(\bar{V}$=0.5)	$\|\mathbf{S}\|^2(\bar{V}$=0.0)
0	0.5	0.0	1.06E-03	0.0	1.0
1	0.5	0.0	2.51E-04	0.0	1.0
2	1.5	0.0	1.08E-03	0.0	1.0
1	1.5	0.0	3.06E-04	0.0	1.0
2	2.5	0.0	1.25E-03	0.0	1.0
3	2.5	0.0	1.50E-04	0.0	1.0
4	3.5	0.0	1.14E-03	0.0	1.0
3	3.5	0.0	2.61E-04	0.0	1.0
...	...	...	...	...	...

Table 2: The modules of S-matrix for neutron partial waves with varying imaginary potentials, where $\bar{V}$ is the scaled depth defined as $\frac{V_i(new)}{V_i(old)}$.

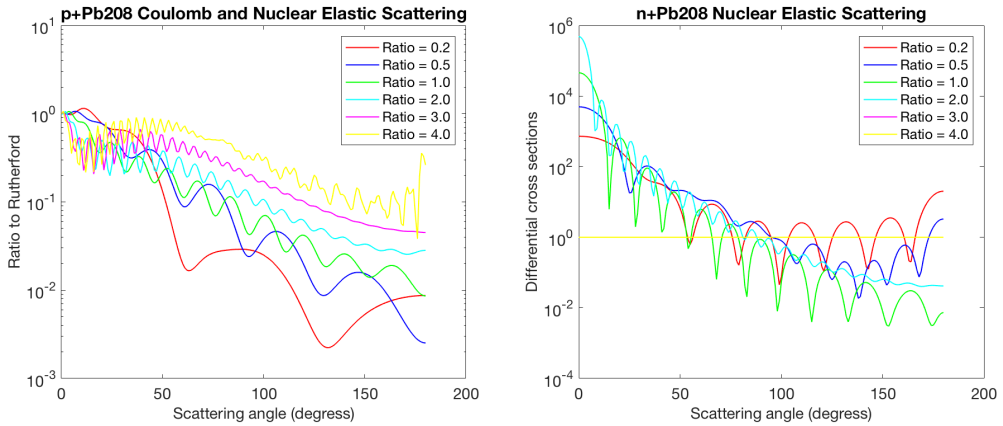

Figure 2: Differential cross sections for nucleons scattering with ^{208}Pb with different radius parameters at 50MeV, where ratio is defined as $\frac{r_{new}}{r_{old}}$. Left panel is proton and right panel is neutron

References

[1] Ian J Thompson and Filomena M Nunes. Nuclear reactions for astrophysics: principles, calculation and applications of low-energy reactions. pages 62–64,129–131, 2009.

[2] I.J. Thompson. Fresco, coupled reaction channels calculations. `http://www.fresco.org.uk/`. Accessed Feb 25, 2018.

[3] Roberto Capote, Michel Herman, P Obložinskỳ, PG Young, Stéphane Goriely, T Belgya, AV Ignatyuk, Arjan J Koning, Stéphane Hilaire, Vladimir A Plujko, et al. Ripl–reference input parameter library for calculation of nuclear reactions and nuclear data evaluations. *Nuclear Data Sheets*, 110(12):3107–3214, 2009.

[4] AJ Koning and JP Delaroche. Local and global nucleon optical models from 1 kev to 200 mev. *Nuclear Physics A*, 713(3-4):231–310, 2003.